

Design and Characterization of Amino and Chloro Functionalized Rhombohedral Silsesquioxanes

Ahmet GÜLTEK¹, Turgay SEÇKİN^{1*}, Halil İbrahim ADIGÜZEL²

¹*İnönü University, Faculty of Arts and Science, Chemistry Department,
Malatya 44280, TURKEY
e-mail: tseckin@inonu.edu.tr*

²*İnönü University, Faculty of Arts and Science Physics Department,
Malatya 44280, TURKEY*

Received 14.05.2004

A more rapid and a versatile synthetic approach for the preparation of polyhedral silsesquioxanes (POSS) by hydrolytic condensation of organosilicon monomers in the presence of a Pt catalyst was studied. The structural properties of POSS molecules were determined by X-ray powder diffraction analysis, yielding a rhombohedral unit cell with $a = 11,52796\text{Å}$ and $\alpha = 94,9754^\circ$ for octaaminopropyl-POSS, and a rhombohedral unit cell with $a = 11,51421\text{Å}$, $\alpha = 96,7214^\circ$ for octachloropropyl-POSS. The activation energies were found to be 64.8, and 89.1 kJ/mol for octaaminopropyl-POSS and octachloropropyl-POSS, respectively. The products were also characterized by Fourier transform infrared spectroscopy, ¹H and ¹³C nuclear magnetic resonance, differential thermal analysis, and thermogravimetric analysis.

Key Words: Ceramics, Sol-gel; POSS, activation energy, Kissinger Equation.

Introduction

Sol-gel chemistry allowed the emergence of the synthesis of organopolysilsesquioxanes having a well defined three-dimensional network due to the presence of covalent bonds between organic and inorganic fragments, and the so-called hybrid materials.

Our research concerns the synthesis of polyhedral oligomeric silsesquioxane (POSS) by the sol-gel chemistry. While several processes for the production of POSS molecules or nano particles derived from functional silanes appeared recently^{1–16}.

One of the most extensively studied systems, involving the preparation of polyhedral oligomeric silsesquioxane, is their derivative^{16–21}. The results of experimental and theoretical studies of these systems suggest that the morphology is governed by three effects; the type of the organosilane, the solvent, and the catalyst^{22–27}.

*Corresponding author

While the first two factors are now usually taken into account in both experimental and theoretical studies, the literature dealing with the process conditions remain very scarce, mainly because of the lack of experimental data on the process conditions of controlled morphology²⁸.

In this work, we try to partially fill this gap by giving a method of preparation of POSS from γ -aminopropyltrimethoxy silane (APS), and γ -chloropropyltrimethoxy silane (CLS) in the presence of a catalyst. In this work our objective is three fold: (1) to give the experimental conditions to prepare the POSS framework, (2) to elucidate the structure by means of X-ray diffraction (XRD) studies, Fourier transform infrared spectroscopy (FT-IR), and ¹³C- and ¹H nuclear magnetic resonance (NMR) spectroscopy. (3) to compare the thermo chemistry of POSS prepared from APS and CLS, by thermogravimetry and differential thermal analysis (DTA).

Experimental

All reactions were performed under an atmosphere of dry nitrogen using standard Schlenck techniques; reagent grade chemicals were used without further purifications unless noted. The following reagents were purchased from Fluka: γ -aminopropyltrimethoxysilane (CLS), γ -chloropropyltrimethoxysilane (APS), and PtCl₄. An ultra-pure water filtering system was used to produce deionized water, and methanol was dried over calcium hydride.

Preparation of POSS-CLS and POSS-NH₂

In each sol-gel polymerization, the monomer solutions and the monomer and catalyst solutions (200 ppm by weight) were sealed in polypropylene bottles, the product was washed with H₂O (3x100 ml) and ether (2x50 ml) and dried under vacuum for 24h at 100 °C.

A solution of CLS or APS 45 ml was added in a solution of dry methanol. To this mixture was added 28 ml concentrated HCl, and the reaction mixture was kept at room temperature for 2 days. PtCl₄ was added to this solution as catalyst in an argon atmosphere. The reaction mixture was transferred to the Schlenck and heated to 50 °C. A crystalline precipitate formed after a day at 50 °C, was collected and treated as described above. The product has a melting point of 207-208 °C and 220-222 °C for POSS-CLS and POSS-NH₂ respectively.. And the chlorine content was found to be 27.6 % wt. The GPC chromatogram indicated monodisperse compounds. The ¹H-NMR and ¹³C NMR (DMSO-d₆) spectra are given in Table 1.

Table 1. ¹H-NMR and ¹³C NMR (DMSO-d₆) spectra of POSS-NH₂ and POSS-CLS(δ referenced to the residual solvent CDCl₃).

	¹ H NMR (δ^a ppm)	¹³ C-NMR (δ^a ppm)
POSS-NH ₂ .8HCl	8.28 (s, 24 H, NH ₂); 2.70 (t, CH ₂ N, 16H); 1.61 (m, SiCH ₃ CH ₃ ,16H); 0.61 (t, SiCH ₂ , 16H).	47.01 (s, CH ₂ N); 22.61 (s, SiCH ₂ CH ₂) 9.44 (s, SiCH ₂)
POSS- NH ₂	5.3 (s, NH ₂); 2.70 (t, CH ₂ N, 16H); 2.42 (m, SiCH ₃ CH ₃ ,16H); 0.74 (t, SiCH ₂ , 16H).	48.87 (s, CH ₂ N); 28.88 (s, SiCH ₂ CH ₂) 10.5 (s, SiCH ₂)
POSS-CLS	1.81 (m, SiCH ₃ CH ₃ ,16H); 0.91 (t, SiCH ₂ , 16H)	27.3 (s, SiCH ₂ CH ₂) 8.57 (s, SiCH ₂)

^a Chemical Shift in part per million (ppm).

Procedure for the determination of the amino content

The content of amino groups of the POSS framework was determined by consumption of HCl aqueous solutions. In a typical procedure, into a 100 ml flask, 0.10 g of POSS-NH₂ and 20 ml of 0.01 mol/l HCl aqueous solution were charged, and the mixture was stirred at room temperature for two days, filtrated, and the filtrate was back titrated with NaOH (aq) using an indicator. Then the amount of terminal amino groups per 1.0 g POSS-NH₂ was calculated to be 15.2 %.

Characterization

The thermal behavior was studied by DTA (Shimadzu System 50) and TGA (Shimadzu System 50). FT-IR analysis was performed on a Mattson 1100 FT-IR mode spectrometer. ¹H NMR spectra (300.131 MHz) and ¹³C NMR spectra (75.5 MHz) were measured on a Bruker AM 300 WB FT spectrometer with δ referenced to the residual solvent CDCl₃. Microanalyses were performed by TÜBİTAK (Ankara). The structural investigation of a composite material thus prepared was carried out at room temperature by the Rigaku System RadB X-ray diffractometer was employed a Cu radiation with the scan rate of 1°/min.

Results and Discussion

The hybrid solids POSS-CLS and POSS-NH₂ were prepared upon hydrolysis of CLS and APS under PtCl₄ catalysis. The solid which formed quantitatively was recovered by filtration and washed successively with H₂O, and ether. After drying, the solid was collected as white powder.

From DTA analysis, the exothermic crystallization peak shifts to lower temperatures as decreasing the heating rate. A simple and convenient method is to use several heating rates such as, 5, 10, 15, 20 and 25 K/min, and then extrapolation to an infinitesimal heating rate can be performed. As shown in Figure 1, the exothermic peak temperature at 356 °C corresponds to the loss of organic segment, whereas the exothermic peaks temperatures at 432 and 564 °C are attributed to the phase transition temperatures. The DTA and TGA thermogram are shown in Figure 2, the peak at 421 °C corresponds the loss of organic segments. The peak at 591 °C was assigned to the phase transition. All evidences were supported by TGA analysis. The difference in peak temperature is due to the molecular symmetry, and molecular rearrangement is more likely to take place in POSS-NH₂ via hydrogen bonding.

The activation energy of crystallization of both systems was determined by Kissinger equation²⁹ (Figs. 3 and 4). The relation between the crystalline peak temperature T_p and heating rate β is indicated by

$$\ln(\beta/T_p^2) = -E_Q/RT_p + A \quad (1)$$

where E_Q is the activation energy of the reaction, R is the gas constant, and A is a constant.

The activation energies associated with one crystallization peak can be derived from the plot as 64.8 and 89.1 kJ/mol for POSS-NH₂, and POSS-CLS, respectively. The higher activation energy observed for POSS-CLS reflects the stabilization of the phase as compared with POSS-NH₂.

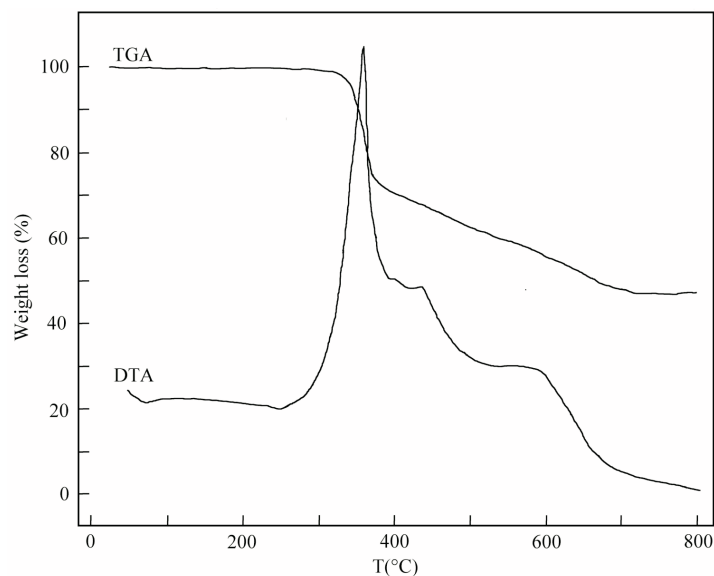


Figure 1. The DTA and TGA thermogram of POSS-NH₂ 10K/min in air atmosphere.

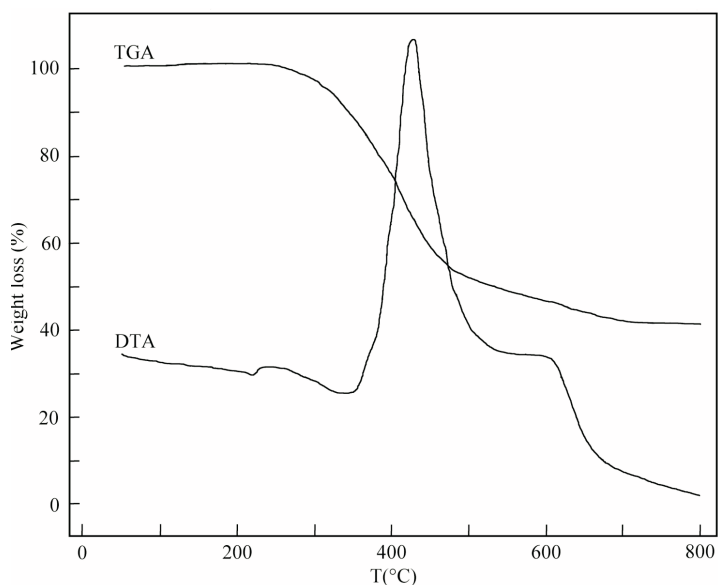


Figure 2. The DTA and TGA thermogram of POSS-CLS 10K/min in air atmosphere.

TGA plot for the prepared POSS frameworks are shown in Figures 1 and 2, respectively. The presence of distinctive mass-loss regions at 421 and 356 °C for POSS-CLS, and POSS-NH₂, respectively, suggest that a complicated process took place in both cases that might be the result of the structural transformation. The initial weight loss for POSS-CLS occurs at 300 °C and is fully subsided by 470 °C. The same trend was observed for POSS- NH₂ as well. The initial weight loss appearing at 350 °C indicated organic segments have been decomposed, is fully subsided at 375 °C.

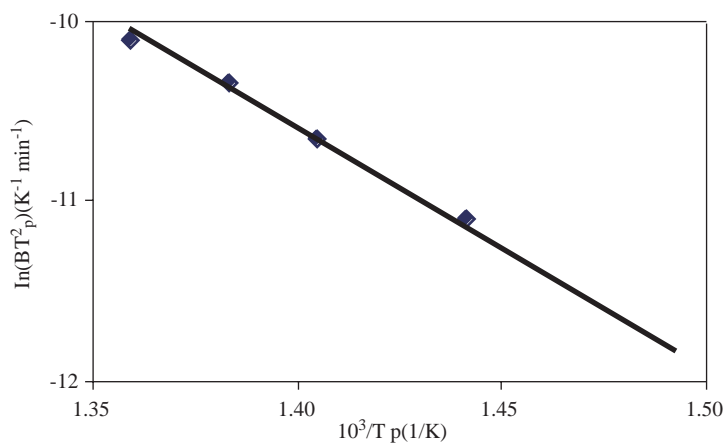


Figure 3. Kissinger plot of the crystallization peak temperature (POSS-NH₂) T_p taken from DTA curves of different heating rates.

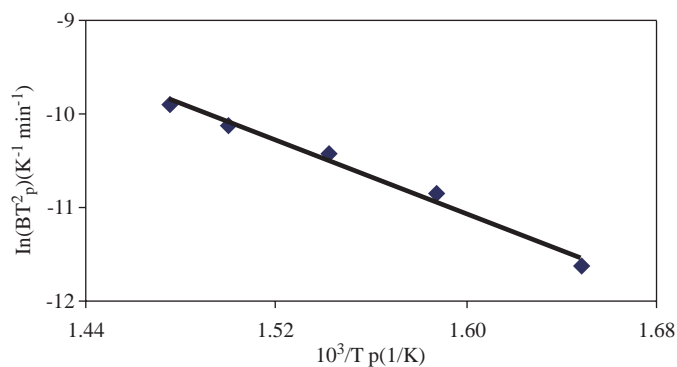


Figure 4. Kissinger plot of the crystallization peak temperature (POSS-CLS) T_p taken from DTA curves of different heating rates.

The ¹H and ¹³C NMR spectra results are given in Table 1. The data are well suited with the proposed structure in which rhombohedral unit cell formation is likely to taken place. The POSS framework was accomplished by hydrolytic condensation of APS and CLS with the appropriate amount of PtCl₄. The amount of catalyst was a crucial for the ease of preparation, because it was rationalized that without the catalyst the end of the reaction takes longer times, for a week to a month to accomplish the formation of the products.

Octachloro substituted framework has proper melting point; octaaminosubstituted framework sublimes above 400 °C. We have chosen APS and CLS as starting material for two reasons: (i) it is commercially available, and (ii) it has a functional end, which can be linked to a variety of organic groups to prepare novel materials. The FT-IR spectra of both frameworks are shown in Figures 5 and 6. The tentative assignments for the spectra of the frameworks were as follows: 1174 cm⁻¹ (asymmetrical) ν_{as} (Si-O-Si), 1060 cm⁻¹ ν (Si-O-), 938 and 785 cm⁻¹ (symmetrical) ν_s (Si-O-Si), 620 and 550 cm⁻¹ ν_s (Si-O-Si). Polysiloxanes made up tetrahedral (T) units, [RSiO_{1.5}]_x, showed a broad, structureless absorption covering the entire region of 1160–1000 cm⁻¹.

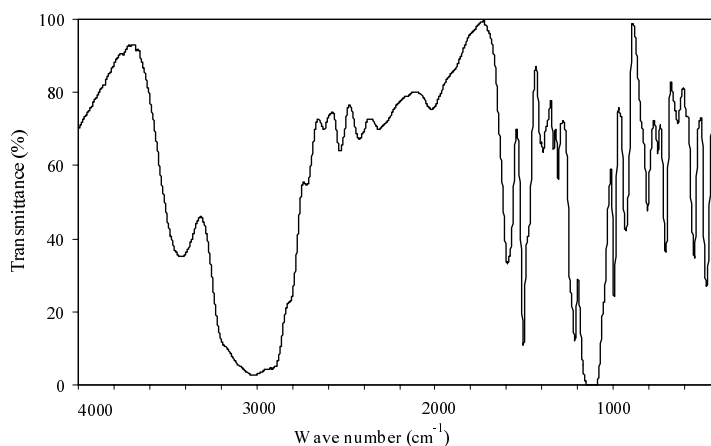


Figure 5. FT-IR spectra of POSS-NH₂ framework.

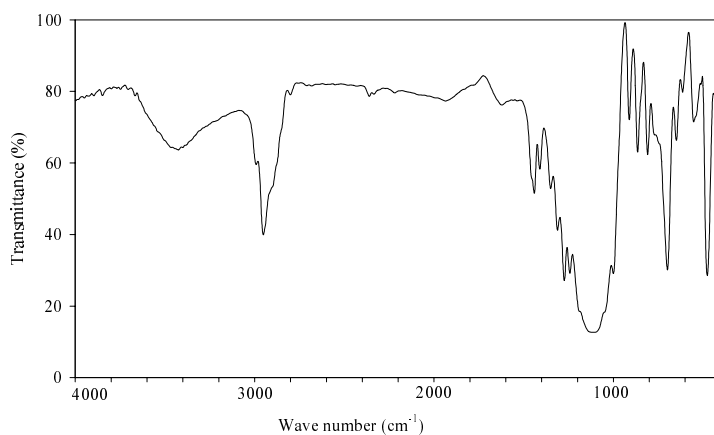


Figure 6. FT-IR spectra of POSS-CLS framework.

The XRD patterns of POSS-NH₂ and POSS-CLS are shown in Figures 7 and 8, respectively. The observed pattern for POSS-NH₂ and POSS-CLS can be fitted to a rhombohedral unit cell as given in Table 2 and 3.

The X-ray powder diffraction profile of POSS-NH₂ and POSS-CLS are indexed by rhombohedral unit cell with $a = 11,52796 \text{ \AA}$, $\alpha = 94,9754 \text{ \AA}$ with the volume of $1513,6 \text{ \AA}^3$ and $1492,32$ respectively. The peak analysis in all POSS hybrids can be attributed to the rhombohedral unit cell formation as expected in the presence of POSS inorganic segments. From the analysis of the XRD spectrum we conclude that all samples showed higher crystallization evidenced by sharp peaks, however some amorphous character was also observed. This findings might be attributed to the Si-O-Si linkages indicating that high degree of crystall character due to the rigid network caused by both POSS segment.

The above observations show that the synthesis of the hybrid solid, which results, from the formation of strong Si-O-Si bonds, is controlled by intermolecular interactions of precursor molecules during the hydrolysis and condensation of $(RO)_3Si-R'$. The structural differences between two precursors probably result from controlled condensation reaction, owing to the interactions developing between monomeric units. $PtCl_4$ catalysis which leads to a slow and moderate condensation of the silicate units probably facilitate the ordering of the organic fragments owing to the rigidity of siloxane network that differs in POSS-CLS and POSS-NH₂.

Table 2. Observed and calculated 2θ value using a rhombohedral cell with $a = 11.52796 \text{ \AA}$ and $\alpha = 94,9754^\circ$ and volume = $1513,6 \text{ \AA}^3$ the measured diffraction intensity from the X-ray powder diffraction pattern obtained from POSS- NH_2 .

2θ obs (deg)	2θ calc. (deg)	Error (%)	hkl
7,727	7,727	0.000	100
18,693	19,06	0,367	21-1
20,52	20,46	-0,058	211
23,30	23,32	+0,023	300
25,28	25,30	+0,026	310
26,82	26,83	+0,014	-320
27,34	27,37	+0,029	311
31,28	31,27	-0,011	400
33,06	33,04	-0,021	41-1

Table 3. Observed and calculated 2θ values using a rhombohedral unit cell with $a = 11.51421 \text{ \AA}$, $\alpha = 96.7214^\circ$ and volume = $1492,32 \text{ \AA}^3$ the measured diffraction intensity from the X-ray powder diffraction pattern obtained from POSS-CLS.

2θ obs (deg)	2θ calc. (deg)	Error (%)	hkl
7,794	7,794	0.000	100
10,28	10,27	-0.009	110
11,90	11,74	-0.158	110
18,68	18,73	+0.054	211
22,10	22,08	-0,020	122
28,20	28,20	+0,006	311

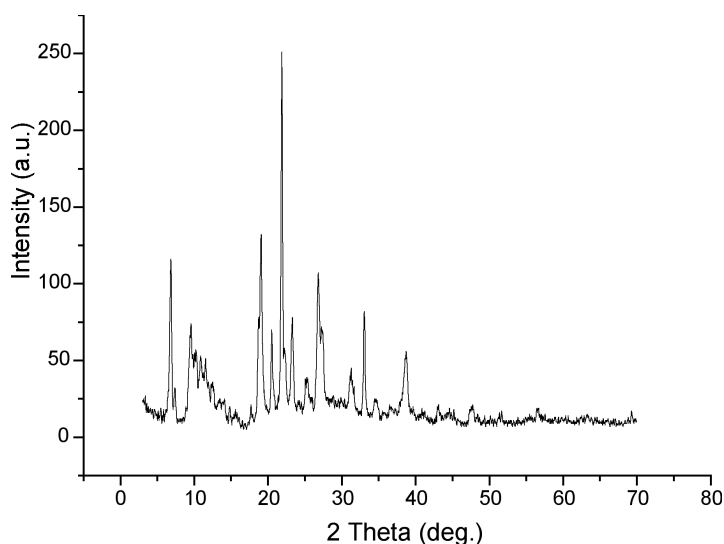


Figure 7. The X-ray powder diffraction profile of POSS- NH_2 . The crystal can be indexed by rhombohedral unit cell with $a = 11,52796 \text{ \AA}$, $\alpha = 94,9754^\circ$.

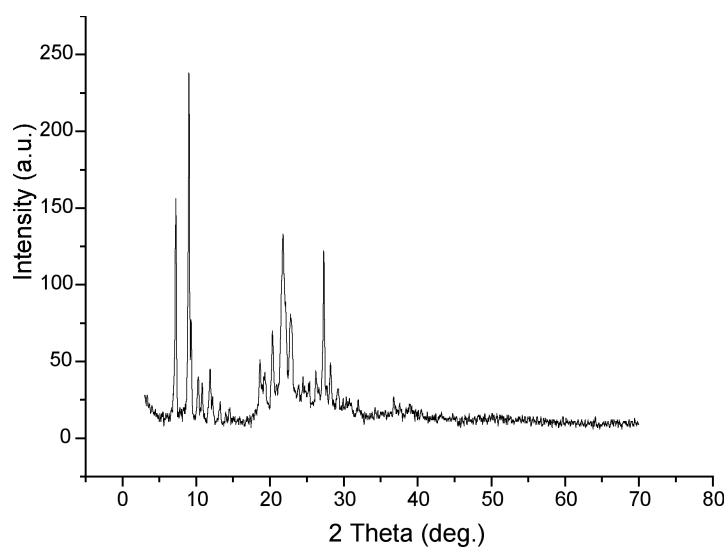


Figure 8. The X-ray powder diffraction profile of POSS-CLS. The crystal can be indexed by rhombohedral unit cell with $a = 11,51421\text{\AA}$, $\alpha = 96,7214^\circ$.

Conclusions

We have investigated the structural variation of POSS framework from γ -aminopropyltrimethoxysilane and γ -chloropropyltrimethoxysilane in terms of thermal behaviour and activation energies. The structural elucidation was made with x-ray diffractometer and found to be rhombohedral in the case of POSS-NH₂ and POSS-CLS respectively. Thermal studies revealed that the activation energies are 64.6 and 89,1 kJ.

References

1. F.J. Feher, D. Soulivong, A.G. Eklund, **Chem. Commun.** 399-400 (1998).
2. F.J. Feher, D. Soulivong, F.Nguyen, **Chem. Commun.** 1279-1280 (1998).
3. F.J. Feher, K.D. Wyndham, D.J. Knauer, **Chem. Commun.** 2393-2394 (1998).
4. F.J. Feher, K.D. Wyndham, M.A. Scialdone, Y.Hamuro, **Chem. Commun.** 1469-1470 (1998).
5. F.J. Feher, D. Soulivong, A.G. Eklund, K.D. Wyndham, **Chem. Commun.** 1185-1186 (1997).
6. R.A. Mantz, P.F. Jones, K.P. Chaffe, J.D. Lichtenhan, J.W. Gilman, **Chem. Mater.** **8**, 1250-1259 (1996).
7. F.J. Feher, D. Soulivong, G.T. Lewis, **J. Am. Chem. Soc.** **119**, 11323-11324 (1997).
8. A. Lee, J.D. Lichtenhan, **Macromolecules** **31**, 4970-4974 (1998).
9. F.J. Feher, K.D. Wyndham, **Chem. Commun.** 323-324 (1998).
10. A.N. Marui, C.C. Riccardi, **Polymer Bulletin** **45**, 523-530 (2001).
11. A. Sellinger, R.M. Laine, **Chem. Mater.** **8**, 1592-1593 (1996).
12. F.J. Feher, S.H. Phillips, J.W. Ziller, **J. Am. Chem. Soc.** **119**, 3397-3398 (1997).
13. C. Zhang, F. Babonneau, C.Bonhemme, R.M.Laine, C.L.Soles, H.A.Hristov, A.F. Yee, **J. Am. Chem. Soc.** **120**, 8380-8391 (1998).

14. T. Kudo, M.S. Gordon, **J. Am. Chem. Soc.** **120**, 11432-11438 (1998).
15. A. Sellinger, R.M. Laine, **Macromolecules** **29**, 2327-2330 (1996).
16. T.S. Haddad, J.D. Lichtenhan, **Macromolecules** **29**, 7302-7304 (1996).
17. A. Tsuchida, C. Bolln, F.G. Sernetz, H. Frey, R. Mülhaupt, **Macromolecules** **30**, 2818-2824 (1997).
18. J.L. Hedrick, H.J. Cha, R.D. Miller, D.Y. Yoon, H.R. Brown, S. Srinivasan, R.D. Pietro, R.F. Cook, J.P. Hummel, D.P. Klaus, E.G. Liniger, and E.E. Simonyi **Macromolecules** **30**, 8512-8515 (1997).
19. A. Lee, J.D. Lichtenhan, **Macromolecules** **31**, 4970-4974 (1998).
20. B.R. Harkness, K. Takeuchi, M. Tachikawa, **Macromolecules** **31**, 4798-4805 (1998).
21. D.P. Fasce, R.J.J. Williams, F. Mechin, J.P. Pascault, M.F. Llauro, R. Petiaud, **Macromolecules** **32**, 4757-4763 (1999).
22. J. Pyun, K. Matyjaszewski, **Macromolecules** **33**, 217-220 (2000).
23. P. Eisenberg, R. Erra-Balsells, Y. Ishikawa, J.C. Lucas, A.N. Mauri, H. Nonami, C.C. Riccardi, R.J.J. Williams, **Macromolecules** **33**, 1940-1947 (2000).
24. V. Chandrasekhar, R. Murugavel, A. Voigt, H.W. Roesky, H.G. Schmidt, M. Noltemeyer, **Organometallics** **15**, 918-922 (1996).
25. A. Klemp, H.W. Roesky, H.G. Schmidt, H.S. Park, M. Noltemeyer, **Organometallics** **17**, 5225-5227 (1998).
26. R. Duchateau, H.C.L. Abbenhuis, R.A. van Santen, S.K.H. Thiele, M.F.H. van Tol, **Organometallics** **17**, 5222-5224 (1998).
27. R. Duchateau, U. Cremer, R.J. Harmsen, S.I. Mohamud, H.C.L. Abbenhuis, R.A. van Santen, A. Meetsma, S.K.H. Thiele, M.F.H. van Tol, M. Kranenburg, **Organometallics** **18**, 5447-5459 (1999).
28. R. Duchateau, R.A. van Santen, G.P.A. Yap, **Organometallics** **19**, 809-816 (2000).
29. H.E. Kissinger, **Anal. Chem.** **29**, 1702 (1957).